marine drugs

MDPI

Article

Steroids from the Deep-Sea-Derived Fungus *Penicillium granulatum* MCCC 3A00475 Induced Apoptosis via Retinoid X Receptor (*RXR*)-α Pathway

Chun-Lan Xie [1,2,†], Duo Zhang [1,†], Jin-Mei Xia [2], Chao-Chao Hu [1], Ting Lin [1], Yu-Kun Lin [2], Guang-Hui Wang [1], Wen-Jing Tian [1], Zeng-Peng Li [2], Xiao-Kun Zhang [1,*], Xian-Wen Yang [2,*] and Hai-Feng Chen [1,*]

1 School of Pharmaceutical Sciences, Xiamen University, South Xiangan Road, Xiamen 361005, China; xiechunlanxx@163.com (C.-L.X.); 32320151154210@stu.xmu.edu.cn (D.Z.); 32320171153261@stu.xmu.edu.cn (C.-C.H.); linting@xmu.edu.cn (T.L.); guanghui@xmu.edu.cn (G.-H.W.); tianwj@xmu.edu.cn (W.-J.T.)

2 Key Laboratory of Marine Biogenetic Resources, South China Sea Bio-Resource Exploitation and Utilization Collaborative Innovation Center, Third Institute of Oceanography, Ministry of Natural Resources, 184 Daxue Road, Xiamen 361005, China; xiajinmei@tio.org.cn (J.-M.X.); yukunlin223@163.com (Y.-K.L.); lizengpeng@tio.org.cn (Z.-P.L.)

* Correspondence: xkzhang@xmu.edu.cn (X.-K.Z.); yangxianwen@tio.org.cn (X.-W.Y.); haifeng@xmu.edu.cn (H.-F.C.); Tel.: +86-592-2181851 (X.-K.Z.); +86-592-2195319 (X.-W.Y.); +86-592-592-2187225 (H.-F.C.)

† These authors contributed equally to this work.

Received: 24 February 2019; Accepted: 15 March 2019; Published: 19 March 2019

Abstract: Five new ergostanes, penicisteroids D−H (**1**−**5**), were isolated from the liquid culture of the deep-sea-derived fungus *Penicillium granulatum* MCCC 3A00475, along with 27 known compounds. The structures of the new steroids were established mainly on the basis of extensive analysis of 1D and 2D NMR as well as HRESIMS data. Moreover, the absolute configurations of **1** were confirmed unambiguously by the single-crystal X-ray crystallography. Compounds **2** and **4**–**7** showed moderate antiproliferative effects selectively against 12 different cancer cell lines with IC_{50} values of around 5 μM. Compounds **2** and **6**, potent *RXRα* binders with Kd values of 13.8 and 12.9 μM, respectively, could induce apoptosis by a Retinoid X Receptor (*RXR*)-α-dependent mechanism by regulating RXRα transcriptional expression and promoting the poly-ADP-ribose polymerase (PARP) cleavage. Moreover, they could inhibit proliferation by cell cycle arrest at the G0/G1 phase.

Keywords: marine-derived fungus; *Penicillium granulatum*; ergostanes; anti-tumor; nuclear receptor

1. Introduction

Retinoid X receptor-α (*RXRα*), one of the most promising members of the nuclear receptor superfamily, plays an important role for the treatment of cancer, metabolic, and neurodegenerative diseases [1–4]. It can form heterodimers with retinoic acid retinoid (*RAR*), thyroid hormone receptor (*TR*), nerve growth factor-induced gene B (*NGFIB*), etc. [5,6]. As a matter of fact, thirteen percent of all Food and Drug Administration (FDA)-approved drugs are targeting nuclear receptors [7,8]. In 1999, the retinoid X receptor (*RXR*) agonist, targretin™ (bexarotene), was approved by the FDA for the treatment of cutaneous T-cell lymphoma, stimulating scientists around the world to search for more *RXR* transcriptional inhibitors [9,10].

Penicillium granulatum MCCC 3A00475 was isolated from a deep-sea sediment sample of the Antarctic Ocean. Previously, the chemical investigation on the rice static fermentation extract of

this fungus provided novel spiro-diterpenoids, alkaloids, and steroids [11,12]. Inspired by OSMAC (One-Strain Many Compounds) strategy, the fungus was subjected to further investigation using different fermentation conditions. Interestingly, under the agitated fermentation in liquid medium, its secondary metabolic profile changed dramatically. Moreover, the crude extract showed potent cytotoxicity against several cancer cells. Therefore, a large-scale fermentation was conducted, followed by a systematic chemical isolation. As a result, five new and 27 known compounds were obtained (Figure 1). Compounds **2** and **4**–**7** showed moderate inhibitory effects selectively against 12 different cancer cell lines with IC_{50} values of around 5 μM. The mechanism study indicated they could not only induce apoptosis through an RXRα-dependent pathway but also inhibit the proliferation by cell cycle arrest at G0/G1 phase. Herein, we report the isolation, structure elucidation, and cytotoxicity against a panel of cancer cell lines of these compounds.

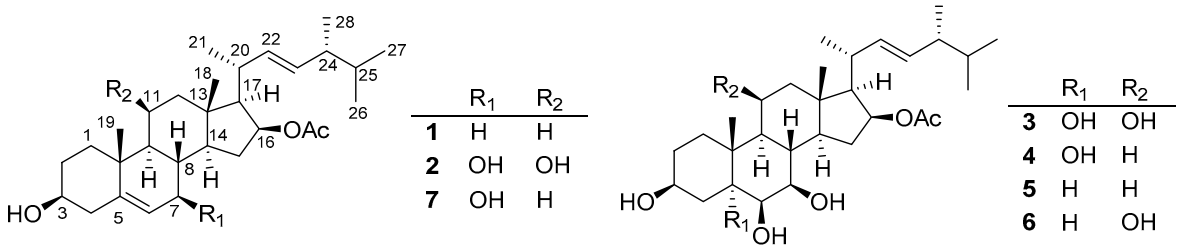

Figure 1. Chemical structures of **1**−**7** isolated from *Penicillium granulatum* MCCC 3A00475.

2. Results and Discussion

Compound **1** was isolated as colorless needle crystals. The sodium adduct molecular ion peak at *m/z* 479.3547 in the HRESIMS (High Resolution Electrospray Ionization Mass Spectroscopy) indicated its molecular formula as $C_{30}H_{48}O_3$, requiring six degrees of unsaturation. The ^{1}H NMR spectrum (Figure S1) exhibited four methyl doublets [δ_H 0.82 (3H, d, J = 6.7 Hz, Me-26), 0.84 (3H, d, J = 6.7 Hz, Me-27), 0.87 (3H, d, J = 6.9 Hz, Me-28), 1.06 (3H, d, J = 6.7 Hz, Me-21)], three methyl singlets [δ_H 0.93 (3H, s, Me-18), 1.03 (3H, s, Me-19), and 1.98 (3H, s, Me-2′)], three olefinic protons [δ_H 5.32 (1H, d, J = 5.0 Hz, H-6), 5.19 (2H, m, H-22 and H-23)], and two oxymethine [δ_H 3.38 (1H, m, H-3), 5.00 (1H, dt, J = 7.6, 3.6 Hz, H-16)]. The ^{13}C and DEPT (Distortionless Enhancement by Polarization Transfer) spectra (Figure S2) revealed the presence of 30 carbons, including seven sp^3 methyls, seven methylenes, twelve methines (two oxygenated sp^3 and three sp^2), and four non-protonated carbons (two sp^2 and two sp^3). Altogether, the 1D NMR spectroscopic data (Tables 1 and 2) indicated one acetoxyl moiety [δ_H 1.98 (3H, s, Me-2′); δ_C 172.3 (s, C-1′), 21.7 (q, Me-2′)] and a 28-carbon skeleton. Since four olefinic carbons and one carboxyl moiety accounted for three unsaturation degrees, **1** should be a tetracyclic molecule. The assumption, along with the presence of four methyl doublets and two methyl singlets, suggested a steroid skeleton for **1**.

In the COSY (Correlation Spectroscopy) spectrum (Figure S4), a long chain was constructed according to correlations from H-3 (δ_H 3.38 m) via H-4 at δ_H (2.20 m) to the allyl proton H-6 (δ_H 5.32, d, J = 5.0 Hz), and subsequently to H-7 (δ_H 1.93, ddd, J = 12.3, 5.2, 2.2 Hz)/H-8 (δ_H 1.48 m)/H-14 (δ_H 1.0 m)/H-15 (δ_H 2.30 m and 1.02 m)/H-16 (δ_H 5.00, dt, J = 7.6, 3.6 Hz)/H-17 (δ_H 1.29 m)/H-20 (δ_H 2.53 m)/H-22 (δ_H 5.19 m), from H-3 via H-2 (δ_H 1.45 m) to H-1 (δ_H 1.08 dd, J = 13.2, 3.9 Hz), from H-8 via H-9 (δ_H 0.96 m) to H-11 (δ_H 1.57 m)/H-12 (δ_H 2.04, dt, J = 12.5, 3.3 Hz; 1.28 m), and from H-20 to Me-21 (δ_H 1.06, d, J = 6.7 Hz). In addition, another fragment could be deduced by the COSY correlations from two methyl doublets of Me-26 and Me-27 via H-25 (δ_H 1.40 m) to H-24 (δ_H 1.76 m), while H-24 to H-23 (δ_H 5.19 m) and Me-28 (Figure 2). Since the chemical shifts of the two sp^2 methine protons were overlapped at δ_H 5.19 (m), the above deduced two fragmentations could not be connected according to the COSY spectrum. However, it could be easily resolved by the HMBC (Heteronuclear Multiple-bond Correlation) cross peaks of H-20, H-24, Me-21, and Me-28 (Figure S5). Furthermore, the HMBC correlations of two methyls of Me-18 and Me-19 constructed four rings of the

steroid skeleton. In addition, the connection of the acetoxyl moiety to C-16 was proved by the HMBC correlation of H-16 to the carboxyl carbon at δ_C 172.3. On the basis of the above evidence, the planar structure of **1** was then assigned as 16-acetoxy-3-hydroxyergost-5,22*E*-diene, the 7-dehydroxy derivate of penicisteroid A [13].

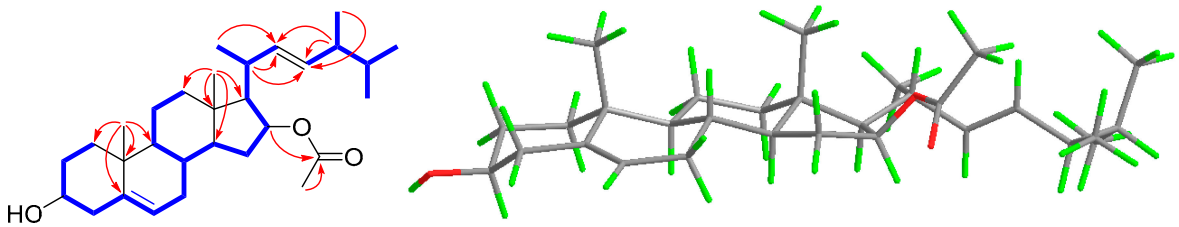

Figure 2. Key COSY (—), HMBC (⌒), and NOESY (⌒) correlations of **1.**

Table 1. ^{1}H NMR data of **1**−**5** at 400 MHz in CD_3OD (δ in ppm, J in Hz within parentheses).

No.	1	2	3	4	5
1	1.86 dt (13.2, 3.5); 1.08 dd (13.2, 3.9)	1.98 m; 1.17 m	1.95 m; 1.28 m	1.54 m; 1.31 m	1.63 m; 0.93 m
2	1.77 m; 1.45 m	1.80 m; 1.54 m	1.75 m; 1.56 m	1.75 m; 1.48 m	1.73 m; 1.40 m
3	3.38 m	3.41 m	3.98 m	3.99 m	3.53 m
4	2.20 m	2.27 m	2.17 dd (13.1, 11.4); 1.57 m	2.07 dd (13.0, 11.6); 1.58 m	1.76 m; 1.56 m
5					1.13 m
6	5.32 d (5.0)	5.14 br s	3.37 d (4.5)	3.37 d (4.1)	3.55 m
7	1.93 ddd (12.3, 5.2, 2.2); 1.53 m	3.75 br d (7.3)	3.68 dd (9.8, 4.6)	3.68 dd (10.2, 4.1)	3.16 dd (10.1, 3.6)
8	1.48 m	1.87 m	1.94 m	1.67 m	1.69 m
9	0.96 m	1.10 m	1.54 m	1.41 m	0.73 dt (12.1, 4.6)
11	1.57 m	4.27 dt (3.6, 2.9)	4.12 m	1.42 m	1.58 m; 1.42 m
12	2.04 dt (12.5, 3.3); 1.28 m	2.23 dd (14.2, 2.2); 1.37 dd (14.1, 3.6)	2.20 dd (13.7, 2.6); 1.33 m	2.01 dt (12.7, 3.1); 1.17 m	2.00 m; 1.16 m
14	1.00 m	1.08 m	1.15 m	1.17 m	1.13 m
15	2.30 m, 1.02 m	2.54 m; 1.44 m	2.62 ddd (7.8, 7.6, 6.9); 1.48 m	2.58 m; 1.42 m	2.62 m; 1.43 m
16	5.00 dt (7.6, 3.6)	5.01 dt (7.8, 4.5)	5.00 dt (7.8, 4.5)	5.00 dt (7.8, 4.2)	4.99 dt (7.9, 4.4)
17	1.29 m	1.22 dd (11.1, 7.8)	1.19 dd (10.8, 7.7)	1.21 m	1.22 m
18	0.93 s	1.16 s	1.14 s	0.92 s	0.93 s
19	1.03 s	1.33 s	1.31 s	1.14 s	1.06 s
20	2.53 m	2.54 m	2.52 m	2.52 m	2.53 m
21	1.06 d (6.7)	1.09 d (6.6)	1.08 d (6.8)	1.05 d (6.8)	1.06 d (6.8)
22	5.19 m	5.19 m	5.18 m	5.19 m	5.19 m
23	5.19 m	5.19 m	5.18 m	5.19 m	5.19 m
24	1.76 m	1.75 m	1.78 m	1.76 m	1.75 m
25	1.40 m	1.41 m	1.41 m	1.42 m	1.40 m
26	0.82 d (6.7)	0.82 d (6.7)	0.82 d (6.8)	0.82 d (7.0)	0.82 d (7.0)
27	0.84 d (6.7)	0.84 d (6.7)	0.83 d (6.7)	0.84 d (7.0)	0.84 d (7.0)
28	0.87 d (6.9)	0.87 d (6.7)	0.87 d (6.8)	0.87 d (6.8)	0.87 d (6.9)
2′	1.98 s	1.98 s	1.98 s	1.97 s	1.97 s

The relative configuration of **1** was established according to the coupling constants and NOESY (Nuclear Overhauser Effect) spectrum (Figure S6). The chair conformations of rings A and B and a trans-relationship between them were established by the large half-peak-width of H-3 (W1/2 = 15.9 Hz) as well as the NOESY correlations of Me-19 to H-1a (δ_H 1.86)/H-2a (δ_H 1.45)/H-8 (δ_H 1.48), Me-18 to H-8/H-12a (δ_H 2.04), while H-3 to H-1b (δ_H 1.08)/H-2b (δ_H 1.77) (Figure 2). However, the terrible overlapped signals of H-9 (δ_H 0.96 m)/H-14 (δ_H 1.00 m)/H-15a (δ_H 1.02 m) and H-12a (δ_H 1.28 m)/H-17 (δ_H 1.29 m) make it impossible to establish its relative configuration. Fortunately, an orthorhombic crystal was obtained from MeOH. By the single X-ray diffraction analysis using Cu–Kα radiation(Tables S1–S4), the absolute configurations of C-3

and C-16 were both assigned as *S* (Figure 3). Accordingly, **1** was unambiguously established as 16*β*-acetoxy-3*β*-hydroxyergost-5,22*E*-diene and named penicisteroid D.

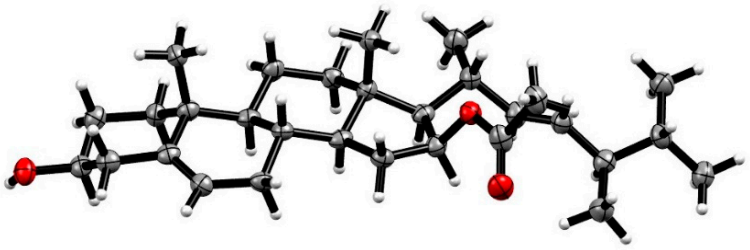

Figure 3. The single X-ray crystallography of **1**.

Table 2. ^{13}C NMR spectroscopic data for **1**—**5** at 100 MHz in CD_3OD (δ in ppm).

No.	1	2	3	4	5
1	38.5 CH_2	37.1 CH_2	33.2 CH_2	33.5 CH_2	39.7 CH_2
2	32.3 CH_2	32.1 CH_2	31.5 CH_2	31.7 CH_2	32.1 CH_2
3	72.4 CH	71.6 CH	69.0 CH	68.0 CH	72.3 CH
4	43.0 CH_2	41.8 CH_2	41.3 CH_2	41.7 CH_2	36.1 CH_2
5	142.3 C	146.0 C	77.9 C	77.8 C	47.4 CH
6	122.2 CH	125.5 CH	78.8 CH	79.3 CH	76.1 CH
7	32.8 CH_2	74.1 CH	74.2 CH	73.3 CH	77.4 CH
8	32.8 CH	38.2 CH	36.3 CH	39.1 CH	38.6 CH
9	51.7 CH	54.2 CH	48.4 CH	45.4 CH	53.9 CH
10	37.7 C	38.0 C	39.5 C	38.8 C	35.9 C
11	21.9 CH_2	68.4 CH	68.0 CH	22.2 CH_2	22.0 CH_2
12	40.9 CH_2	49.9 CH_2	50.2 CH_2	41.3 CH_2	41.0 CH_2
13	43.6 C	43.3 C	44.0 C	44.8 C	44.7 C
14	56.0 CH	57.0 CH	56.6 CH	54.9 CH	54.9 CH
15	36.0 CH_2	37.5 CH_2	38.6 CH_2	38.7 CH_2	38.8 CH_2
16	77.1 CH	77.1 CH	77.5 CH	77.6 CH	77.7 CH
17	61.2 CH	61.2 CH	61.2 CH	60.5 CH	60.4 CH
18	13.1 CH_3	15.4 CH_3	15.8 CH_3	13.4 CH_3	13.3 CH_3
19	20.6 CH_3	22.8 CH_3	20.1 CH_3	17.6 CH_3	16.4 CH_3
20	35.9 CH	35.8 CH	35.9 CH	35.8 CH	35.8 CH
21	21.5 CH_3	21.5 CH_3	21.6 CH_3	21.6 CH_3	21.5 CH_3
22	136.8 CH	136.9 CH	137.0 CH	137.0 CH	136.9 CH
23	133.9 CH	133.7 CH	133.7 CH	133.7 CH	133.7 CH
24	44.8 CH	44.7 CH	44.8 CH	44.8 CH	44.7 CH
25	34.3 CH	34.3 CH	34.3 CH	34.3 CH	34.3 CH
26	19.9 CH_3	20.1 CH_3	20.6 CH_3	20.1 CH_3	20.1 CH_3
27	20.2 CH_3	20.5 CH_3	20.7 CH_3	20.6 CH_3	20.5 CH_3
28	18.7 CH_3	18.6 CH_3	18.6 CH_3	18.6 CH_3	18.6 CH_3
1′	172.3 C	170.1 C	172.4 C	172.4 C	172.4 C
2′	21.7 CH_3	21.7 CH_3	21.7 CH_3	21.7 CH_3	21.6 CH_3

Compound **2** was isolated as an amorporous powder. The molecular formula, $C_{30}H_{48}O_5$, was assigned by the sodium adduct molecular ion peak at *m/z* 511.3383 in the HRESIMS, indicating six degrees of unsaturation. The ^{1}H and ^{13}C NMR spectra (Figures S7 and S8) exhibited 30 carbons, including four doublet and three singlet methyls, five methylenes, 14 methines (four oxygenated and three olefinic), and four non-protonated carbons (one olefinic and one carboxyls). These signals were closely similar to those of **1** except for two additional hydroxyls in **2**. In the COSY spectrum (Figure S10), correlations were found of H-8 via the oxymethine proton at δ_H 3.75 to H-6 and via H-9 to another oxymethine proton at δ_H 4.27, suggesting connections of hydroxyls at C-7 and C-11 positions, respectively. Further confirmation was found by the HMBC correlations of H-7 to C-5/C-6/C-8/C-9 and H-11 to C-8/C-9/C-10 (Figure S11). The large coupling constant of $J_{H7,H8}$

(J = 7.3 Hz) was indicative of its axial α-orientation and the small coupling constants of $J_{H9,H11;H11,H12}$ (J = 3.6, 2.9 Hz) pointed to its axial-orientation. This was confirmed by the NOESY correlations of H-9 to H-7/H-11, H-7 to H-14, and H-8 to Me-18/Me-19 (Figure S12). Accordingly, **2** was established as 16β-acetoxy-3β,7β,11β-trihydroxyergost-5,22-diene and named penicisteroid E.

Compound **3** had a molecule formula of $C_{30}H_{50}O_7$ as deduced from the sodium adduct molecular ion at *m/z* 545.3454 $[M+Na]^+$ in the HRESIMS. Its ^1H and ^{13}C NMR spectroscopic data (Figures S13 and S14) greatly resembled those of penicisteroid C [14], expect that an additional hydroxy group was found at the C-5 position. The assumption was confirmed by the HMBC correlations (Figure S17) of Me-19 to C-5 at δ_C 77.9 and by the COSY cross peaks (Figure S16) of H-6 (δ_H 3.37 d, J = 4.5 Hz) via H-7 (δ_H 3.68 dd, J = 9.8, 4.6 Hz) to H-8 (δ_H 1.94 m). By detailed analysis of the HSQC, COSY, HMBC, and NOESY (Figure S18) spectra, **3** was then determined as 16β-acetoxy-3β,5α,6β,7β,11β-pentahydroxyergost-22*E*-ene and named penicisteroid F.

The molecular formula of **4** was determined as $C_{30}H_{50}O_6$ based on the sodium adduct ion peak in its HRESIMS spectrum. The ^1H and ^{13}C NMR spectroscopic data (Figures S19 and S20) of **4** were close similar to those of **3** except that the oxygenated methine (δ_C 68.0) at the C-11 position in **3** was replaced by the methylene (δ_C 22.2) in **4**, suggesting the absence of the hydroxyl group at C-11. This assumption was evidenced by the significant upshift of C-12 from δ_C 50.2 to δ_C 41.3 and C-9 from δ_C 48.4 to δ_C 45.4. Further confirmation was obtained by the COSY correlations (Figure S22) of H-12 (δ_H 2.01 dt, J = 12.7, 3.1 Hz) to H-11 (δ_H 1.42 m). Accordingly, **4** was defined as 16β-acetoxy-3β,5α,6β,7β-tetrahydroxyergost-22*E*-ene, and named penicisteroid G.

Compound **5** was isolated as a white powder. The molecular formula of $C_{30}H_{50}O_5$ was assigned according to the sodium adduct ion peak at *m/z* 513.3570 in its HRESIMS spectrum. Comparison of the ^1H and ^{13}C NMR spectra (Figures S25 and S26) of **5** and **4** showed they were very similar except that the oxygenated non-protonated carbon (δ_C 77.8) at the C-5 position in **4** was replaced by a methine moiety (δ_C 47.4) in **5**. This was evidenced by the HMBC correlations (Figure S29) from H-19 (δ_H 1.06) to C-1 (δ_C 39.7), C-5 (δ_C 47.4), C-9 (δ_C 53.9), and C-10 (δ_C 35.9). Thus, **5** was established as 16β-acetoxy-3β,6β,7β-trihydroxyergost-22*E*-ene, and named penicisteroid H.

By comparison of the NMR and MS data with those published in the literature, 27 known compounds were determined to be penicisteroid A (**6**) [13], penicisteroid C (**7**) [14], anicequol (**8**) [15], ergosta-7,22-diene-3β,5α,6β,9α-tetraol (**9**) [16], (22*E*,24*R*)-3β,5α-trihydroxy- ergost-7,22-dien-6-one (**10**) [17], (3β,5α,6β,22*E*)-ergosta-7,22-diene-3,5,6-triol (**11**) [18], (3β,5α,6β,22*E*)-6-methoxyergosta-7,22-diene-3,5-diol (**12**) [18], 5α,6α,8α,9α-diepoxy-(22*E*,24*R*)-ergoxt-22-ene-3β,7β-diol (**13**) [19], ergosterol peroxide (**14**) [20], ergosterol (**15**) [21], topsentisterol D3 (**16**) [22], (24*S*)-24-ethylcholesta-3β,5α-diol-6-one (**17**) [23], (24*S*)-24-ethylcholesta-3β,5α,6α-triol (**18**) [23], incisterol A2 (**19**) [24], conidiogenones B (**20**) [25], conidiogenone G (**21**) [25], conidiogenone D (**22**) [26], conidiogenone C (**23**) [26], conidiogenones I (**24**) [26], meleagrin (**25**) [27], roquefortine C (**26**) [12], roquefortine F (**27**) [28], (5*S*)-5-(1H-indol-3-ylmethyl)-2,4-imidazolidione (**28**), sorbicillin (**29**) [29], 2′,3′-dihydrosorbicillin (**30**) [30], trichodimerol (**31**) [31], and dihydrotrichodimerol (**32**) [31].

All 19 steroids (**1**–**19**) were tested for cytotoxicity against 12 cancer cell lines of SHG-44, HepG2, A549, BIU-87, BEL-7402, ECA-109, Hela-S3, PANC-1, SW620, HcT116, MCF-7, and MB-231. They showed selectively cytotoxicity against A549, BIU-87, BEL-7402, ECA-109, Hela-S3, and PANC-1 cells. However, none exhibited antiproliferative effect against SW620, HcT116, MCF-7, and MB-231 cancer cell lines (Table 3). Further investigation by flow cytometry (Figure 4) and the Western blotting (Figure 5) indicated compounds **2** and **4**–**7** could induce apoptosis in A549 cells. Moreover, compounds **2** and **6** could also inhibit cell proliferation by cell cycle arresting at G0/G1 phase (Figure 6).

Table 3. The antiproliferative effects (IC_{50}) of compounds **1-19** from *Penicillium granulatum* MCCC 3A00475 against 12 tumor cells [a].

No.	SHG-44	HepG2	A549	BIU-87	BEL-7402	ECA-109	Hela-S3	PANC-1
2	8.3	NA	5.5	NA	NA	NA	NA	NA
4	4.8	6.7	8.0	14.4	8.5	8.3	10.0	5.6
5	NA	7.0	4.4	8.5	NA	9.2	7.2	NA
6	12.5	6.2	4.5	7.7	8.8	4.1	4.8	4.2
7	7.8	NA	4.4	NA	NA	6.6	9.9	7.0
8	NA	NA	5.9	NA	NA	15.6	NA	NA
9	NA	NA	NA	NA	NA	NA	NA	NA
12	NA	NA	7.0	8.7	8.0	NA	NA	6.3
13	NA	NA	NA	NA	NA	7.1	9.8	NA
19	NA	16.6	NA	NA	7.9	7.5	8.2	NA
OT[b]	NA	NA	NA	NA	NA	NA	NA	NA

[a] Twelve tumor cells included SHG-44 (human glioma cell line), HepG2 (liver hepatocellular cell line), A549 (human non-small cell lung cancer cell line), BIU-87 (human bladder cancer cell line), BEL-7402 (human hepatocellular cell line), ECA-109 (human esophageal cancer cell line), Hela-S3 (Human cervical cancer cell line), PANC-1 (Human pancreatic cancer cell line), SW620 (human colon cancer cell line), HcT116 (human colon cancer cell line), MCF-7 (human breast cancer cell line), and MB-231 (human breast cancer cell line). Compounds **1-19** did not show positive effect against four tumor cells of SW620, HcT116, MCF-7, and MB-231 (IC_{50} > 20 μM). [b] Other compounds, including **1**, **3**, **10**, **11**, and **14–18**. NA: No activity was observed (IC_{50} > 20 μM).

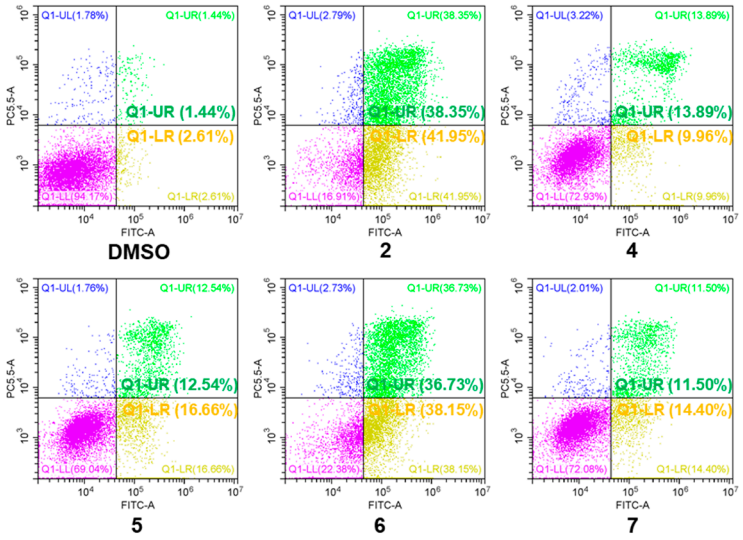

Figure 4. Apoptosis effects of **2** and **4–7** in A549 cells. A549 cells were treated with the tested compounds (50 μM) for 9 h. Then they were stained using the Fluorescein Isothiocyanate (FITC) Annexin V Apoptosis Detection Kit and were analyzed by flow cytometry (FCM). Q1-UR: viable apoptotic cells, Q1-LR: non-viable apoptotic cells, Q1-LL: normal cells, Q1-UL: necrotic cells, and the percentage of QI-UR panel indicates the effect of apoptosis.

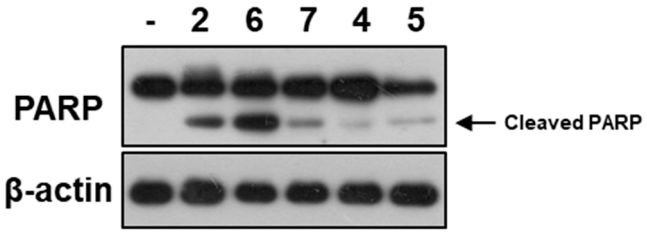

Figure 5. PARP cleavage induced by **2** and **4–7**. A549 cells were treated with the tested compounds (50 μM) for 12 h. The cleaved PARP indicated the apoptosis bioactivity.

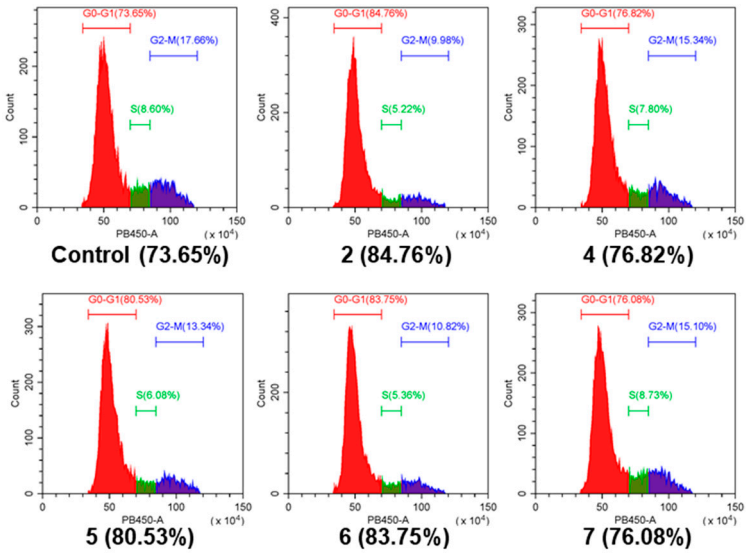

Figure 6. Cell cycle analysis of **2** and **4**–**7**. A549 cells were treated with the tested compounds (25 μM) for 48 h and were stained by 4′6-Diamidino-2-phenylindole dihydrochloride (DAPI). The first red peak indicates cells in the phase G0–G1, the percentages of which are shown next to the group label, and results show the proportion of cells arresting G0-G1 phase increased after treating with compounds **2** and **6**.

To further investigate the apoptosis mechanisms, **2** and **6** were tested for transcriptional activities on two nuclear receptors, *RXRα* and *Nur77* (also called *NGFIB*), using the dual-luciferase reporter gene assay. However, they did not display positive effects on *Nur77*. Instead, they could significantly decrease the transcriptional activation of *RXRα* induced by 9-cis (Figure 7) in a dose-dependent manner (Figure 8). It indicated that **2** and **6** might have selectivity effected transcriptional activation of nuclear receptors and only acted on *RXRα*.

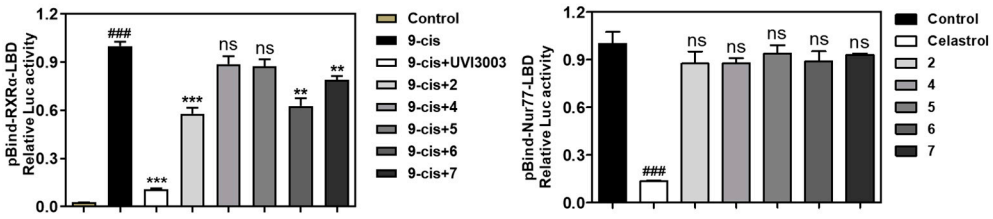

Figure 7. The transcriptional activities of *RXRα* and *Nur77* for **2** and **4**–**7**. (**Left**) Human renal epithelial cells HEK293T transfected dual-luciferase reporter plasmids pBind-*RXRα*-LBD and PG5 were treated with *RXRα* ligand 9-cis-Retinoic acid (9-cis, 0.1 μM), *RXRα* antagonist 3-[4-Hydroxy-3-[5,6,7,8-tetrahydro-5,5,8,8-tetramethyl-3-(pentyloxy)-2-naphthalenyl]phenyl]-2-propenoic acid (UVI3003, 2 μM) and the tested compounds (50 μM) for 18 h, respectively. The luciferase activity of the 9-cis group is normalized to 1. (**Right**) HEK293T cells transfected pBind-*Nur77*-LBD and PG5 plasmids were treated with the tested compounds (50 μM) for 24 h. The luciferase activity of the control group is normalized to 1. ### $p < 0.001$ versus control, ns: no significance, ** $p < 0.01$, *** $p < 0.001$ versus the 9-cis group.

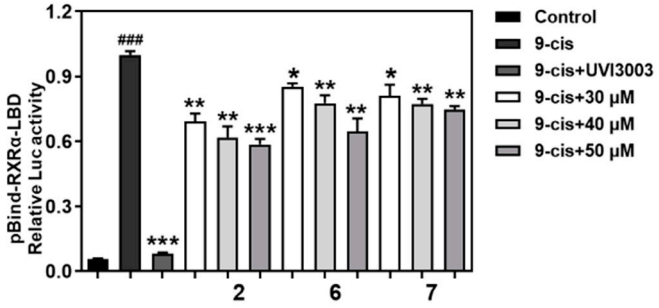

Figure 8. Effects of compounds **2**, **6**, and **7** on the transcriptional activities of *RXRα*. HEK293T cells transfected pBind-*RXRα*-LBD and PG5 plasmids were treated with 9-cis (0.1 μM), UVI3003 (2 μM), and different concentrations of the tested compounds (30, 40, and 50 μM) for 18 h, respectively. The luciferase activity of the 9-cis group is normalized to 1. ### $p < 0.001$ versus control, * $p < 0.05$, ** $p < 0.01$, *** $p < 0.001$ versus the 9-cis group.

Furthermore, we used fluorescence quenching assay (Figure 9) to analyze compounds for binding to *RXRα*-LBD and identified compounds **2** and **6** as a potent binder with a Kd of 13.8 μM and 12.9 μM, and the role of *RXRα* was illustrated by data showing that transfection of *RXRα* small interfering RNA (si-RNA), which inhibited *RXRα* expression, abrogated the apoptosis effect induced by compounds **2** and **6** (Figure 10). The above findings indicated that these compounds might have a useful impact on *RXRα*-mediated growth inhibition and apoptosis induction in cancer cells as well as *RXRα*-dependent regulation of gene expression.

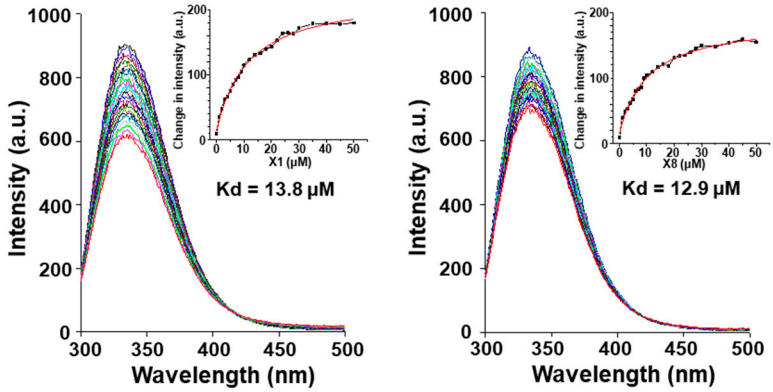

Figure 9. Binding affinity of compounds **2** and **6** to the *RXRα*-LBD. The tested compounds (1–50 μM) were added to the *RXRα*-LBD protein (1 μM in PBS) successively, the fluorescence spectra were obtained from 300 nm to 500 nm using a fluorescence spectrophotometer.

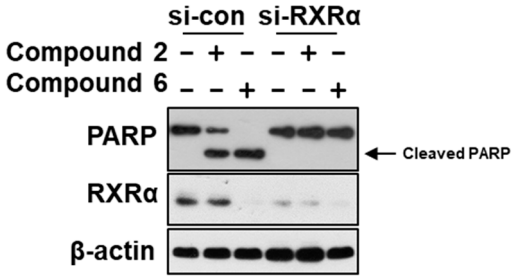

Figure 10. RXRα is required for compounds **2**- and **6**-induced PARP cleavage. A549 cells were transfected with *RXRα* siRNA (SASI_Hs01_00097638, SASI_Hs01_00097639, SASI_Hs01_00097640, Sigma-Aldrich, St. Louis, MO, USA) or control siRNA for 60 h. Then they we1re treated by the tested compound (50 μM) for 12 h, respectively.

3. Materials and Methods

3.1. General Experimental Procedures

Optical rotations were recorded on an MCP 500 automatic polarimeter (Anton Paar Trading Co. Ltd., Shanghai, China) under 20 °C. Ultraviolet spectra were detected by a UV8000 UV/Vis spectrophotometer (Shanghai Metash instrument Co., Ltd., Shanghai, China). The HRESIMS spectra were measured by a Xevo G2 Q-TOF mass spectrometer (Waters Corporation, Milford, MA, USA). The NMR spectra were recorded on a 400 MHz spectrometer (Bruker, Fällanden, Switzerland) using TMS as the internal standard. Reversed-phase HPLC was performed on a 1260 infinity instrument (Agilent Technologies, San Diego, CA, USA) equipped with the DAD detector. Purifications by column chromatography (CC) were performed on silica gel, Sephadex LH-20, and ODS. The TLC plates were visualized under UV light or by spraying with 10% H_2SO_4.

3.2. Fungal Identification, Fermentation, and Extract

The fungus of *Penicillium granulatum* MCCC 3A00475 was provided by the Marine Culture Collection of China (MCCC). The isolation and identification were described previously [11,12].

Erlenmeyer flasks (250 mL) containing 100 mL fermentation media were directly inoculated with a quarter plate of the strain spores. After 2 days of incubation at 28 °C on a rotary shaker at 180 r/min, 20 mL seed cultures were transferred into a total of 100 flasks (1 L) containing 380 mL of defined medium (10 g glucose, 20 mL mannitol, 5 g potato peptone, 5 g monosodium glutamate, 3 g yeast extract, 3 g maltose dissolved in 1 L of water, pH 7.5). The flasks were cultured with shaking at 180 rpm and 28 °C for 11 days.

The culture (40 L) was centrifuged to separate the broth and mycelia. The mycelia were exhaustively extracted with EtOAc (ethyl acetate) three times to yield a dark brown gum (30.0 g).

3.3. Isolation and Purification

The EtOAc extract was subjected to CC on silica gel by gradient $CHCl_3$–MeOH (0→100%) as solvents to give eight fractions (Fr.1–Fr.8). Fraction Fr.1 (662.1 mg) was CC over silica gel using petroleum ether (PE)–EtOAc (10:1) to provide **29** (5.7 mg). Fr.2 (694.3 mg) was separated by CC over Sephadex LH-20 (MeOH), followed by purification using prep-HPLC (20→100% MeOH, 20 mm × 25 cm, 10 mL/min) and CC over silica gel (PE-EtOAc, 10:1) to give **1** (4.5 mg), **14** (89.5 mg), **15** (24.6 mg), **18** (1.0 mg), **20** (11.4 mg), **21** (1.4 mg), **22** (4.9 mg), **23** (3.9 mg), and **24** (1.5 mg). Fr.3 (259.6 mg) was CC over Sephadex LH-20 (MeOH). Further purification by prep-HPLC to give **12** (2.5 mg), **16** (1.5 mg), **31** (6.5 mg), and **32** (10.6 mg). Fr.4 (512.2 mg) was separated by CC on Sephadex LH-20 (MeOH), and then by prep-HPLC (40→100% MeOH, 20 mm × 25 cm, 10 mL/min) to afford **8** (9.1 mg) and **25** (134.2 mg). Fr.5 (109.5 mg) was purified by CC on Sephadex LH-20 (MeOH) to obtain **7** (81.9 mg) and **19** (0.5 mg). Fr.6 (586.3 mg) was subjected to CC on Sephadex LH-20 (MeOH) and prep-HPLC (20→80% MeOH, 20 mm × 25 cm, 10 mL/min) to give **2** (12.5 mg), **10** (5.8 mg), **13** (1.4 mg), **26** (4.3 mg), and **27** (5.0 mg). Fr.7 was separated into three sub-fractions (Fr.7.1–Fr.7.3) by CC on Sephadex LH-20 (MeOH). Fr.7.1 (61.5 mg) was purified by preparative HPLC (20→70% MeOH, 10 mm × 25 cm, 5 mL/min) to afford **9** (0.6 mg), **11** (1.8 mg), and **30** (9.7 mg). Fr.7.2 (168.3 mg) was purified by prep-HPLC (30→80% MeOH, 20 mm × 25 cm, 10 mL/min) to provide **5** (1.6 mg) and **6** (58.5 mg). Fr.7.2 (168.3 mg) was purified by prep-HPLC (65% MeOH, 20 mm × 25 cm, 10 mL/min) to give **17** (2.3 mg) and **28** (1.3 mg). Fr.8 (812.4 mg) was CC on Sephadex LH-20 (MeOH) and preparative HPLC (60→100% MeOH, 10 mm × 25 cm, 5 mL/min) to give compound **3** (3.8 mg) and **4** (3.9 mg).

Penicisteroid D (**1**): colorless needle; $[\alpha]_D^{20}$ +0.25 (c 0.32, MeOH); UV (MeOH) λmax (log ε) 203 (2.38) nm; ^1H and ^{13}C NMR data, see Tables 1 and 2; HRESIMS *m/z* 479.3547 $[M + Na]^+$ (calcd for $C_{30}H_{48}O_3Na$, 479.3501).

Penicisteroid E (**2**): amorphous powder; $[\alpha]_D^{20}$ +16.6 (*c* 1.09, MeOH); UV (MeOH) λmax (log ε) 205 (1.69) nm; ^{1}H and ^{13}C NMR data, see Tables 1 and 2; HRESIMS *m/z* 511.3383 $[M + Na]^+$ (calcd for $C_{30}H_{48}O_5Na$, 511.3399).

Penicisteroid F (**3**): white powder; $[\alpha]_D^{20}$ +19.1 (c 0.31, MeOH); UV (MeOH) λmax (log ε) 205 (2.71) nm; ^{1}H and ^{13}C NMR data, see Tables 1 and 2; HRESIMS *m/z* 545.3454 $[M + Na]^+$ (calcd for $C_{30}H_{50}O_7Na$, 545.3454).

Penicisteroid G (**4**): white powder; $[\alpha]_D^{20}$ +10.5 (c 0.08, MeOH); UV (MeOH) λmax (log ε) 204 (2.20) nm; ^{1}H and ^{13}C NMR data, see Tables 1 and 2; HRESIMS *m/z* 529.3518 $[M + Na]^+$ (calcd for $C_{30}H_{50}O_6Na$, 529.3505).

Penicisteroid H (**5**): white powder; $[\alpha]_D^{20}$ +16.8 (c 0.08, MeOH); UV (MeOH) λmax (log ε) 204 (0.57) nm; ^{1}H and ^{13}C NMR data, see Tables 1 and 2; HRESIMS *m/z* 513.3570 $[M + Na]^+$ (calcd for $C_{30}H_{50}O_5Na$, 513.3556).

3.4. X-Ray Crystallographic Analysis of Compound **1**

Compound **1** was obtained as a colorless orthorhombic crystal from MeOH. The crystal data were recorded with an Xcalibur Eos Gemini single-crystal diffractometer with Cu Kα radiation (λ = 1.54184 Å). Space group $P2_12_12_1$, a = 5.94350(10) Å, b = 11.98440(10) Å, c = 38.3459(4) Å, $\alpha = \beta = \gamma = 90^o$, V = 2731.35(6) Å^3, Z = 4, D_{calcd} = 1.111 mg/cm^3; crystals size 0.15 × 0.12 × 0.05 mm^3, μ = 0.533 mm^{-1}, F (000) = 1008; A total of 18,704 reflections were collected in the range of 2.304 to 67.080°, of which 4726 independent reflections [R (int) = 0.0845] were used for analysis. The final R indices [I > 2sigma(I)] R_1 = 0.0797, wR_2 = 0. 2359. The absolute structure parameter was −0.06 (15). Crystallographic data of **2** have been deposited in the Cambridge Crystallographic Data Center (CCDC), with deposition number 1887656. Copies of the data can be obtained, free of charge, on application to CCDC, 12 Union Road, Cambridge CB21EZ, UK, (fax: +44(0)-1233-336033; email: deposit@ccdc.cam.ac.uk).

3.5. Cell Proliferation Assay

Cytotoxic activities of all steroids were conducted on human glioma cell line SHG-44, liver cancer cell lines HepG2, and 7402, non-small cell lung cancer cell line A549, bladder cancer cell line BIU-87, esophageal cancer cell line ECA-109, cervix cancer cell line Hela-S3, pancreatic cancer cell line PANC-1, colon carcinoma cell lines SW620 and HcT116, breast cancer cell lines MCF-7and MB-231 by MTT method as reported previously [32].

3.6. Apoptosis Determination by FCM

The levels of cellular superoxide were assessed by using FITC Annexin V Apoptosis Detection Kit (556547, BD Biosciences, San Diego, CA, USA) according to the manufacturer's instructions. Briefly, A549 cells treated with trypsin and resuspended in Annexin V binding buffer, then the cells were labelled by PI and FITC. At last, fluorescence was measured by flow cytometry using FITC-A (CytoFLEX, Beckman Coulter, Kraemer Boulevard Brea, CA, USA).

3.7. Western Blotting

Cell lysates were boiled in sodium dodecyl sulfate (SDS) sample loading buffer, resolved by 10% SDS–polyacrylamide gel electrophoresis (SDS–PAGE) and transferred to nitrocellulose. The membranes were blocked in 5% milk in Tris-buffered saline and Tween 20 (TBST; 10 mM Tris-HCl (pH 8.0), 150 mM NaCl, and 0.05% Tween 20) for 1 h at room temperature. After washing twice with TBST, the membranes were incubated with appropriate primary antibodies (Anti-PARP, 9542, CST, Boston, Massachusetts, USA; Anti-β-actin, 4970S, CST, Boston, Massachusetts, USA; Anti-*RXRα*, ΔN197, Santa Cruz, 2145 Delaware Ave, CA, USA) in TBST for 1 h and then washed twice, probed with horseradish peroxide-linked anti-immunoglobulin (1:5000 dilution) for 1 h at room temperature. After three washes with TBST, immunoreactive products were visualized using enhanced chemiluminescence reagents and autoradiography.

3.8. Cell Cycle Determination by FCM

A549 cells were treated with trypsin then dehydrated with 70% ethyl alcohol overnight. After washing twice by PBS, the cells were labelled by DAPI (1:10000 in PBS, D8417 from Sigma-Aldrich, Saint Louis, MO, USA). At last, fluorescence was measured by flow cytometry using PB450-A (CytoFLEX, Beckman Coulter, Kraemer Boulevard Brea, CA, USA).

3.9. Dual-Luciferase Reporter Assay

Cells were transfected with the corresponding plasmids for 24 h and then treated with compounds for 12 h. Cells were lysed and luciferase relative activity was tested by the Dual-Luciferase Reporter Assay System according to the manufacturer's instructions. Transfection efficiency was normalized to Renilla luciferase activity. Culture medium DMEM containing 0.5% DMSO was regarded as blank control. Celastrol (1 μM), UVI3003 (2 μM, sc-358586, santa cruz, 2145 Delaware Ave, CA, USA), 9-cis (0.1 μM, R4643, Sigma-Aldrich, St. Louis, MO, USA) were used as positive controls.

3.10. Protein Expression and Purification

The human *RXRα*-LBD was cloned as an N-terminal histidine-tagged fusion protein in pET15b expression vector and overproduced in the *Escherichia coli* BL21 DE3 strain. Briefly, cells were harvested and sonicated, and the extract was incubated with the His60 Ni Superflow resin.

3.11. Fluorescence Quenching Assay

The *RXRα*-LBD protein (1 μM in 3 mL phosphate buffer) was measured with Agilent Technologies Cary Eclipse Fluorescence Spectrophotometer (Agilent Technologies, Malaysia), and the fluorescence spectra were obtained from 300 nm to 500 nm. Compounds were added to the protein. After incubation for 30 s at RT, the incubation buffer was measured with the spectrophotometer. Data were processed and fitted to obtain the binding affinities using Origin (OriginLab, Northampton, MA, USA).

3.12. Statistical Analysis

Each experiment was performed three times. The values shown are the mean ± SD. Student's *t*-test (two-sided) was used to test for significant differences between groups.

4. Conclusions

In conclusion, five new and 27 known compounds were isolated from the deep-sea-derived fungus *Penicillium granulatum* MCCC 3A00475. Compounds **2** and **4**–**7** showed moderate activity against the human lung cancer cell line A549. They could induce PARP cleavage and regulate RXRα transcriptional expression.

Supplementary Materials: The following are available online at http://www.mdpi.com/1660-3397/17/3/178/s1, Figures S1–S30 and Tables S1–S4: The 1D and 2D NMR spectra of **1**−**5** and the X-ray crystallographic data of **1**.

Author Contributions: X.-K.Z., X.-W.Y., and H.-F.C. designed and coordinated the project; C.-L.X., J.-M.X. and Y.-K.L. isolated and purified all compounds. D.Z., C.-C.H., T.L., Z.-P.L. conducted the bioactive experiments. C.-L.X., T.L., G.-H.W., and W.-J.T. analyzed the data. C.-L.X. and X.-W.Y. wrote the paper, while critical revision of the publication was performed by all authors.

Acknowledgments: This work was financially supported by the Xiamen Southern Oceanographic Center (17GYY026NF05), the Science and Technology Research Program of Fujian Province, China (2018N0016), the National Natural Science Foundation of China (U1605221 and 21877022), and the Fundamental Research Funds for the Central University (20720160117).

Conflicts of Interest: The authors declare no conflict of interest.

References

1. Zhang, X.K.; Hoffmann, B.; Tran, P.B.; Graupner, G.; Pfahl, M. Retinoid X receptor is an auxiliary protein for thyroid hormone and retinoic acid receptors. *Nature* **1992**, *355*, 441–446. [CrossRef] [PubMed]
2. Wang, G.H.; Jiang, F.Q.; Duan, Y.H.; Zeng, Z.P.; Chen, F.; Dai, Y.; Chen, J.B.; Liu, J.X.; Liu, J.; Zhou, H.; et al. Targeting truncated retinoid X receptor-α by CF31 induces TNF-α-dependent apoptosis. *Cancer Res.* **2013**, *73*, 307–318. [CrossRef] [PubMed]
3. Su, Y.; Zeng, Z.; Chen, Z.; Xu, D.; Zhang, W.; Zhang, X.K. Recent progress in the design and discovery of RXR modulators targeting alternate binding sites of the receptor. *Curr. Top. Med. Chem.* **2017**, *17*, 663–675. [CrossRef]
4. Chen, F.; Liu, J.; Huang, M.; Hu, M.; Su, Y.; Zhang, X.K. Identification of a New RXRαantagonist targeting the coregulator-binding Site. *Med. Chem. Lett.* **2014**, *5*, 736–741. [CrossRef] [PubMed]
5. Perez, E.; Bourguet, W.; Gronemeyer, H.; de Lera, A.R. Modulation of RXR function through ligand design. *Biochim. Biophys. Acta* **2012**, *1821*, 57–69. [CrossRef]
6. Zhou, H.; Liu, W.; Su, Y.; Wei, Z.; Liu, J.; Kolluri, S.K.; Wu, H.; Cao, Y.; Chen, J.; Wu, Y.; et al. NSAID sulindac and its analog bind RXRα and inhibit RXRα-dependent AKT signaling. *Cancer Cell* **2010**, *17*, 560–573. [CrossRef]
7. Overington, J.P.; Bissan, A.L.; Hopkins, A.L. How many drug targets are there? *Nat. Rev. Drug Discov.* **2006**, *5*, 993–996. [CrossRef]
8. Chen, L.Q.; Aleshin, A.E.; Alitongbieke, G.; Zhou, Y.Q.; Zhang, X.D.; Ye, X.H.; Hu, M.J.; Ren, G.; Chen, Z.W.; Ma, Y. Modulation of nongenomic activation of PI3K signalling by tetramerization of N-terminally-cleaved RXRα. *Nat. Commun.* **2017**, *8*, 16066. [CrossRef]
9. Liu, X.; Tian, W.; Wang, G.; Xu, Q.; Zhou, M.; Gao, S.; Qiu, D.; Jiang, X.; Sun, C.; Ding, R.; et al. Stigmastane-type steroids with unique conjugated $\Delta^{7,9(11)}$ diene and highly oxygenated side chains from the twigs of *Vernonia amygdalina*. *Phytochemistry* **2018**, *158*, 67–76. [CrossRef]
10. Shen, Q.; Dai, Y.; Wang, G.; Yao, F.; Duan, Y.; Chen, H.; Zhang, W.; Zhang, X.; Yao, X. Total synthesis and RXRα-mediated transcription studies of neriifolone B and related compounds. *Bioorg. Med. Chem.* **2014**, *22*, 2671–2677. [CrossRef]
11. Niu, S.; Fan, Z.W.; Xie, C.L.; Liu, Q.; Luo, Z.H.; Liu, G.; Yang, X.W. Spirograterpene A, a tetracyclic spiro-diterpene with a fused 5/5/5/5 ring system from the deep-sea-derived fungus *Penicillium granulatum* MCCC 3A00475. *J. Nat. Prod.* **2017**, *80*, 2174–2177. [CrossRef] [PubMed]
12. Niu, S.; Wang, N.; Xie, C.L.; Fan, Z.; Luo, Z.; Chen, H.F.; Yang, X.W. Roquefortine J, a novel roquefortine alkaloid, from the deep-sea-derived fungus *Penicillium granulatum* MCCC 3A00475. *J. Antibiot.* **2018**, *71*, 658–661. [CrossRef] [PubMed]
13. Gao, S.S.; Li, X.M.; Li, C.S.; Proksch, P.; Wang, B.G. Penicisteroids A and B, antifungal and cytotoxic polyoxygenated steroids from the marine alga-derived endophytic fungus *Penicillium chrysogenum* QEN-24S. *Bioorg. Med. Chem. Lett.* **2011**, *21*, 2894–2897. [CrossRef] [PubMed]
14. Abdel-Razek, A.S.; Hamed, A.; Frese, M.; Sewald, N.; Shaaban, M. Penicisteroid C: New polyoxygenated steroid produced by co-culturing of *Streptomyces piomogenus* with *Aspergillus niger*. *Steroids* **2018**, *138*, 21–25. [CrossRef]
15. Igarashi, Y.; Sekine, A.; Fukazawa, H.; Uehara, Y.; Yamaguchi, K.; Endo, Y.; Okuda, T.; Furumai, T.; Oki, T. Anicequol, a novel inhibitor for anchorage-independent growth of tumor cells from *Penicillium aurantiogriseum* Dierckx TP-F0213. *J. Antibiot.* **2002**, *55*, 371–376. [CrossRef] [PubMed]
16. Yue, J.M.; Chen, S.N.; Lin, Z.W.; Sun, H.D. Sterols from the fungus *Lactarium volemus*. *Phytochemistry* **2001**, *56*, 801–806. [CrossRef]
17. Lee, D.Y.; Lee, S.J.; Kwak, H.Y.; Jung, L.; Heo, J.; Hong, S.; Kim, G.W.; Baek, N.I. Sterols isolated from Nuruk (*Rhizopus oryzae* KSD-815) inhibit the migration of cancer cells. *J. Microbiol. Biotechnol.* **2009**, *19*, 1328–1332. [CrossRef] [PubMed]
18. Chen, S.; Yong, T.; Zhang, Y.; Su, J.; Jiao, C.; Xie, Y. Anti-tumor and anti-angiogenic ergosterols from *Ganoderma lucidum*. *Front. Chem.* **2017**, *5*, 85–96. [CrossRef]
19. Yaoita, Y.; Endo, M.; Tani, Y.; Machida, K.; Amemiya, K.; Furumura, K.; Kikuchi, M. Sterol constituents from seven mushrooms. *Chem. Pharm. Bull.* **2008**, *47*, 847–851. [CrossRef]

20. Lima, G.D.S.; Rocha, A.M.D.; Santos, G.F.D.; D'Silva, A.F.; Marriel, I.E.; Takahashi, J.A. Metabolic response of *aspergillus sydowii* to OSMAC modulation produces acetylcholinesterase inhibitors. *Phytochem. Lett.* **2018**, *24*, 39–45. [CrossRef]
21. Tao, R.; Wang, C.Z.; Kong, Z.W. Antibacterial/antifungal activity and synergistic interactions between polyprenols and other lipids isolated from *Ginkgo biloba* L. leaves. *Molecules* **2014**, *239*, 587–594. [CrossRef]
22. Luo, X.; Li, F.; Shinde, P.B.; Hong, J.; Lee, C.O.; Im, K.S.; Jung, J.H. 26,27-Cyclosterols and other polyoxygenated sterols from a marine sponge *Topsentia* sp. *J. Nat. Prod.* **2006**, *69*, 1760–1768. [CrossRef]
23. Das, B.; Srinivas, V.N.S. Studies on marine chemicals. part IV. Isolation of cholesterol derivatives from the marine sponge *Spirastrella inconstans*. *J. Nat. Prod.* **1992**, *55*, 1310–1312. [CrossRef]
24. Zhang, Y.M.; Liu, B.L.; Zheng, X.H.; Huang, X.J.; Li, H.Y.; Zhang, Y.; Zhang, T.T.; Sun, D.Y.; Lin, B.R.; Zhou, G.X. Anandins A and B, two rare steroidal alkaloids from a marine *Streptomyces anandii* H41-59. *Mar. Drugs* **2017**, *15*, 355–363. [CrossRef]
25. Du, L.; Li, D.; Zhu, T.J.; Cai, S.X.; Wang, F.P.; Xiao, X.; Gu, Q.Q. New alkaloids and diterpenes from a deep ocean sediment derived fungus *Penicillium* sp. *Tetrahedron* **2009**, *65*, 1033–1039. [CrossRef]
26. Gao, S.S.; Li, X.M.; Zhang, Y.; Li, C.S.; Wang, B.G. Conidiogenones H and I, two new diterpenes of cyclopiane class from a marine-derived endophytic fungus *Penicillium chrysogenum* QEN-24S. *Chem. Biodivers.* **2011**, *8*, 1748–1753. [CrossRef]
27. Zheng, C.J.; Sohn, M.J.; Lee, S.; Kim, W.G. Meleagrin, a new fabI inhibitor from *Penicillium chryosogenum* with at least one additional mode of action. *PLoS ONE* **2013**, *8*, e78922. [CrossRef]
28. Zhou, Z.F.; Kurtan, T.; Yang, X.H.; Mandi, A.; Geng, M.Y.; Ye, B.P.; Taglialatela-Scafati, O.; Guo, Y.W. Penibruguieramine A, a novel pyrrolizidine alkaloid from the endophytic fungus *Penicillium* sp. GD6 associated with Chinese mangrove *Buguiera gymnorrhiza*. *Org. Lett.* **2014**, *16*, 1390–1393. [CrossRef]
29. Zhao, P.J.; Li, G.H.; Shen, Y.M. New chemical constituents from the endophyte *streptomyces* species LR4612 cultivated on *Maytenus hookeri*. *Chem. Biodivers.* **2010**, *3*, 337–342. [CrossRef]
30. Maskey, R.P.; Gruen-Wollny, I.; Laatsch, H. Sorbicillin analogues and related dimeric compounds from *Penicillium notatum*. *J. Nat. Prod.* **2005**, *68*, 865–870. [CrossRef]
31. Lee, D.H.; Lee, J.H.; Cai, X.F.; Jin, C.S.; Lee, K.; Hong, Y.S.; Lee, J.J. Fungal metabolites, sorbicillinoid polyketides and their effects on the activation of peroxisome proliferator-activated receptor γ. *J. Antibiot.* **2010**, *37*, 615–620.
32. Yang, X.W.; Zeng, H.W.; Liu, X.H.; Li, S.M.; Xu, W.; Shen, Y.H.; Zhang, C.; Zhang, W.D. Anti-inflammatory and anti-tumour effects of *Abies georgei* extracts. *J. Pharm. Pharmacol.* **2008**, *60*, 937–941. [CrossRef]